

Contact mechanics of the human finger pad under compressive loads

Dzidek, Brygida; Adams, Michael; Andrews, James; Zhang, Zhibing; Johnson, Simon

DOI:

[10.1098/rsif.2016.0935](https://doi.org/10.1098/rsif.2016.0935)

License:

None: All rights reserved

Document Version

Peer reviewed version

Citation for published version (Harvard):

Dzidek, B, Adams, M, Andrews, J, Zhang, Z & Johnson, S 2017, 'Contact mechanics of the human finger pad under compressive loads', *Journal of The Royal Society Interface*, vol. 14, no. 127, 20160935.
<https://doi.org/10.1098/rsif.2016.0935>

[Link to publication on Research at Birmingham portal](#)

Publisher Rights Statement:

Contact mechanics of the human finger pad under compressive loads
Brygida M. Dzidek, Michael J. Adams, James W. Andrews, Zhibing Zhang, Simon A. Johnson
J. R. Soc. Interface 2017 14 20160935; DOI: 10.1098/rsif.2016.0935. Published 8 February 2017

General rights

Unless a licence is specified above, all rights (including copyright and moral rights) in this document are retained by the authors and/or the copyright holders. The express permission of the copyright holder must be obtained for any use of this material other than for purposes permitted by law.

- Users may freely distribute the URL that is used to identify this publication.
- Users may download and/or print one copy of the publication from the University of Birmingham research portal for the purpose of private study or non-commercial research.
- User may use extracts from the document in line with the concept of 'fair dealing' under the Copyright, Designs and Patents Act 1988 (?)
- Users may not further distribute the material nor use it for the purposes of commercial gain.

Where a licence is displayed above, please note the terms and conditions of the licence govern your use of this document.

When citing, please reference the published version.

Take down policy

While the University of Birmingham exercises care and attention in making items available there are rare occasions when an item has been uploaded in error or has been deemed to be commercially or otherwise sensitive.

If you believe that this is the case for this document, please contact UBIRA@lists.bham.ac.uk providing details and we will remove access to the work immediately and investigate.

Electronic Supplementary Material (ESM1)

Contact mechanics of the human finger pad under compressive loads

Brygida Dzidek, Michael Adams, James Andrews, Zhibing Zhang and Simon Johnson

Ellipsoidal cap model for the finger pad: geometry and elastic contact

Ellipsoid geometry of the undeformed finger pad

The finger pad is approximated to an ellipsoidal cap, which may be represented by a quadratic surface that is given in Cartesian coordinates by the following expression:

$$\frac{x^2}{\ell_a^2} + \frac{y^2}{\ell_b^2} + \frac{z^2}{\ell_c^2} = 1,$$

where ℓ_a , ℓ_b and ℓ_c are the semi-axes to the palmar face (i.e. the middle of the finger pad), the distal face and the radial/ulnar faces respectively (see Fig. 1). A convenient parametric set of equations for an ellipsoid is as follows:

$$\begin{aligned} x &= \ell_a \cos(u) \sin(v) \\ y &= \ell_b \sin(u) \sin(v) \\ z &= \ell_c \cos(v). \end{aligned}$$

The two angular coordinates take the following values $u \in [0, 2\pi]$ and $v \in [0, \pi]$. These angles and the Cartesian coordinates are also shown in Fig. 1.

The undeformed mean curvature of an ellipsoid is given by:

$$H_{0g} = \frac{\ell_a \ell_b \ell_c [3(\ell_a^2 + \ell_b^2) + 2\ell_c^2 + (\ell_a^2 + \ell_b^2 - 2\ell_c^2) \cos(2v) - 2(\ell_a^2 - \ell_b^2) \cos(2u) \sin^2 v]}{8[\ell_a^2 \ell_b^2 \cos^2 v + \ell_c^2 (\ell_b^2 \cos^2 u + \ell_a^2 \sin^2 u) \sin^2 v]^{3/2}}. \quad (1)$$

The four faces that make up the ellipsoidal cap of the finger pad are shown in Figs 2 and 3. To describe the mean curvature it is worth considering that contact is likely to be made in the centre of the radial-ulnar line and hence $z = 0$ and $v = \pi/2$. To capture the different contact points only the angle u needs to be defined and, to exemplify the sensitivity to the orientation, the following values of u will be used: 0° , $\pi/6$ (30°), $\pi/4$ (45°), $\pi/3$ (60°) and $\pi/2$ (90°); these angles are shown schematically in Fig. 4.

The relevant values of u will be determined by reference to the gradient of the contacting plane representing the surface of the compression platen. It will depend on the inclination angle of the finger pad support, θ (30° and 45°); the geometry is shown in Fig. 5(a). To be consistent with the coordinate system above, the gradient of the platen in the x - y plane is

$(\pi/2) - \theta$ (see Fig. 5(b)). This provides the required information to compute u assuming that, in the other direction, the plane is parallel to the z axis.

The ellipsoidal equation to determine the gradient along $z=0$ is as follows:

$$\left(\frac{x}{\ell_a}\right)^2 + \left(\frac{y}{\ell_b}\right)^2 = 1.$$

Hence:

$$y = \pm \ell_b \sqrt{1 - \left(\frac{x}{\ell_a}\right)^2}.$$

Differentiating with respect to x yields:

$$\frac{dy}{dx} = \mp \frac{\ell_b x}{\ell_a^2 \sqrt{1 - \left(\frac{x}{\ell_a}\right)^2}}.$$

The following expressions define the axial positions:

$$\begin{aligned} x &= \ell_a \cos(u) \\ y &= \ell_b \sin(u). \end{aligned}$$

The gradient may then be written as:

$$\frac{dy}{dx} = \mp \frac{\ell_b \cos(u)}{\ell_a \sqrt{1 - \cos^2(u)}} = \mp \frac{\ell_b \cot(u)}{\ell_a} = -\cot(\theta).$$

Thus for a given value of θ it possible to solve the above equation for u .

Two approaches are used to determine the semi-axes of the ellipsoid. The simplest method is to measure directly their lengths from the photographic images of the left index finger taken at appropriate angles. The second approach, which would be expected to be more accurate, is to fit an ellipse in each plane (face). Table 1 shows the results.

Table 1: Left index finger pad semi-axes obtained photographically

Measurement approach	Palmar (mm) ℓ_a	Distal (mm) ℓ_b	Radial - Ulnar (mm) ℓ_c
Direct	7.5	14.7	11.8
Ellipse	7.9	13.8	11.8

Using the results of Table 1, the mean radii of curvature, $R_{0g}(=1/H_{0g})$, along the distal-proximal line are computed from Eqn. (1) and given in Table 2 for different values of u . This shows that there are significant differences between the two sets of values. For the finger pad orientations of $\theta = 30^\circ$ and 45° , the mean radii of curvature calculated from Eqn. (1) using the ellipse approach are 18.7 and 13.2 mm respectively.

Table 2: Mean radii of curvature for left index finger pad ellipsoid

u ($^\circ$)	Mean radius of curvature, R_{0g} (mm)	
	Direct	Ellipse
0	41.0	33.3
30	30.2	25.3
45	20.5	18.0
60	12.2	11.6
90	5.5	6.2

The effective contact curvature, H , used in elastic contact mechanics is defined as follows:

$$H = \frac{1}{R} = \frac{1}{R_1} + \frac{1}{R_2},$$

where R is the corresponding effective contact radius of curvature, and R_1 and R_2 are the (undeformed) mean radii of curvatures of surfaces 1 and 2. For the case of the finger pad ellipsoid (surface 1) touching a flat plane (surface 2), the effective contact curvature is equal to the mean curvature of the ellipsoid at the contact point. i.e. $H = H_{0g}$, and the effective contact radius of curvature, R , is equal to the mean radius of curvature of the ellipsoid at the contact point, R_{0g} . i.e. $R = R_{0g} = 1/H_{0g}$.

Contact mechanics of an elastic ellipsoidal body

In the previous section, the contact between finger pad ellipsoid and a flat surface is essentially approximated to that of a sphere with a radius equal to R_{0g} and a flat surface. However, for asymmetric Hertzian contacts the compressive deformation depends on the local radius of curvature, which is a function of the angular coordinate so that it is necessary to make an appropriate correction. This is possible if the contact area is approximated to an ellipse [1]. The indentation distance, ξ , is then related to the compressive force, W , by the following expression:

$$\xi(e) = \left(\frac{9W^2}{16E_{0g}^* R_{0g}} \right)^{1/3} F_1(e),$$

where E_{0g}^* is the reduced Young's modulus and $e = \left(1 - \ell_e^2 / \ell_d^2 \right)^{1/2}$ where ℓ_d is the semi-major axis (of the contact profile) and ℓ_e is the semi-minor axis and

$$F_1(e) = \{F_2(e)\}^{-1} K(e)$$

$$F_2(e) = \left(\frac{4}{\pi e^2} \right)^{1/3} (\ell_e / \ell_d)^{1/2} \left[\left\{ (\ell_d / \ell_e)^2 E(e) - K(e) \right\} \{K(e) - E(e)\} \right]^{1/6},$$

such that $E(e)$ and $K(e)$ are the complete elliptic integrals. $F_1(e)$ is the correction factor to account for the asymmetry and is equal to unity for a spherical contact. Thus the effective corrected value of the radius of curvature is as follows:

$$R_g^{corr} = R_{0g} F_1^3(e). \quad (2)$$

Tables 3 and 4 show the results of a typical set of calculations for a normal force of 2 N. The values of ℓ_d and ℓ_e were obtained by fitting an ellipse to the corresponding fingerprint image with an equal area. Since $F_1(e) \geq 1$, the value of R_{0g} is increased by this correction as shown in Table 4. Consequently, the values are significantly closer to those obtained from the measured loading data.

Table 3: Measured semi-minor and semi-major axes and area of contact ellipse under a normal force of 2 N, together with the values of u obtained from the undeformed geometry

Wedge angle (°)	Semi-major axis ℓ_d (mm)	Semi-minor axis ℓ_e (mm)	Area (mm ²)	u (°)
45	5.3	4.2	69.4	68.3
30	7.4	5.0	116.3	47.6

Table 4: The mean radii of curvature obtained from the undeformed geometry, the corrected effective values and those obtained from the loading data

Wedge angle (°)	R_{0g} (mm)	R_g^{corr} (mm)	R_g (mm)
45	13.2	14.0	14.5
30	18.7	19.9	20.5

The value of R_g^{corr} can be calculated for each applied force and a sensitivity analysis performed to determine the probable error in the computed values. Figs 6a and 6b show the point wise estimates for 45° and 30° respectively. Combining these pointwise estimates it is possible to state the value of R_g^{corr} and their uncertainties as 14.2 ± 0.6 mm for 45° and 20.2 ± 1.5 mm for 30°.

References

[1] Johnson KL. 1985 *Contact mechanics*. Cambridge, UK: Cambridge University Press.

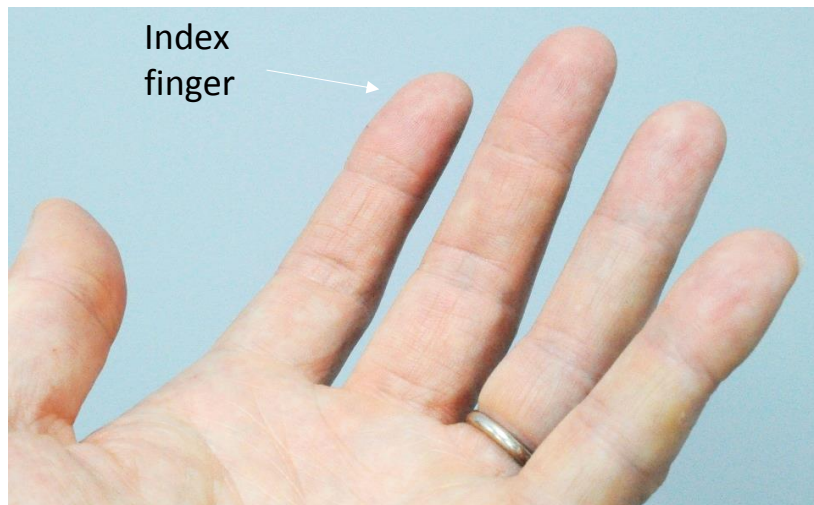
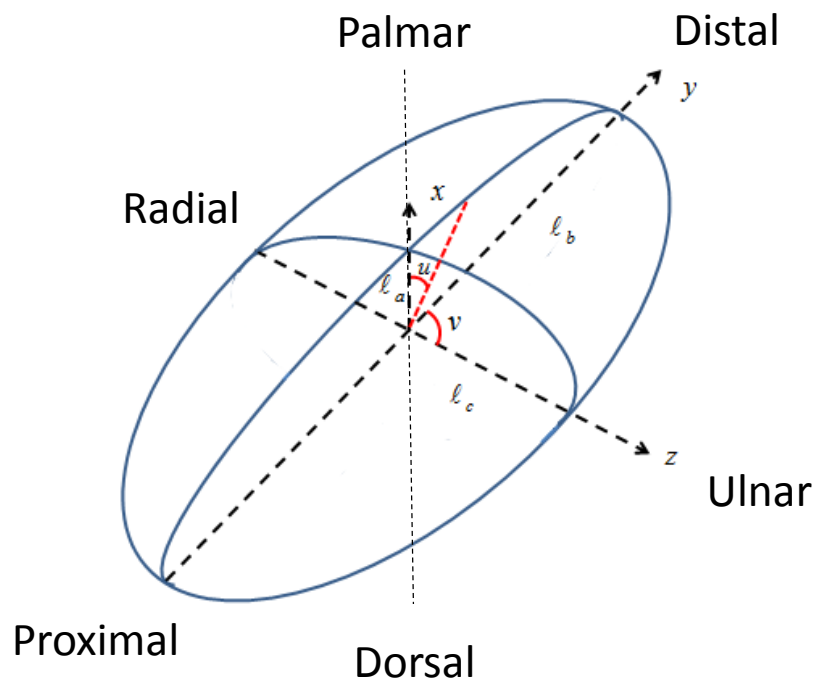


Figure 1: Top view of the ellipsoidal geometry of the finger pad of the index finger of the left hand showing the orientation of the coordinate system.



Figure 2: Schematic diagrams of the index finger of the left hand. Left image: palmar face, middle image: ulnar face, and right image: radial face.

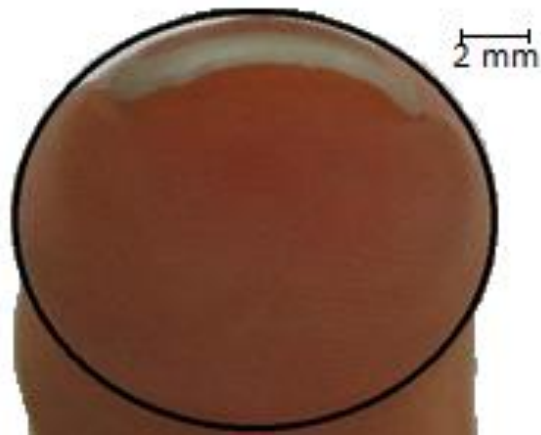


Figure 3: Photograph of the distal face of the index finger of the left hand together with the fitted ellipse.

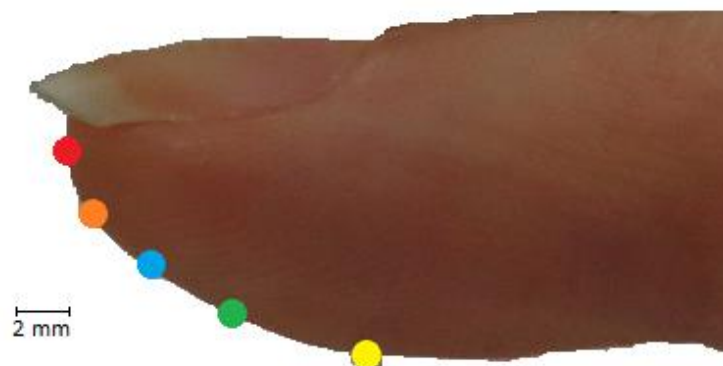
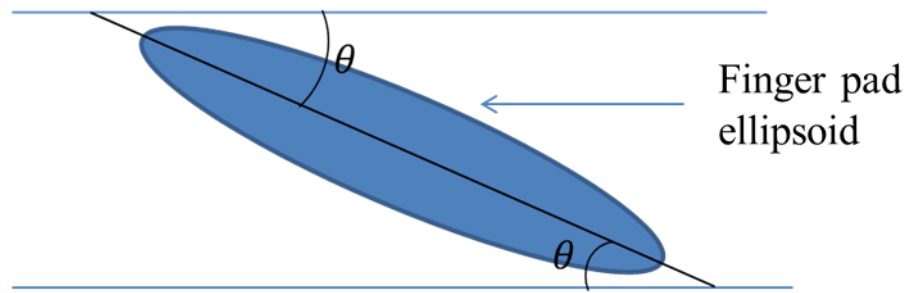
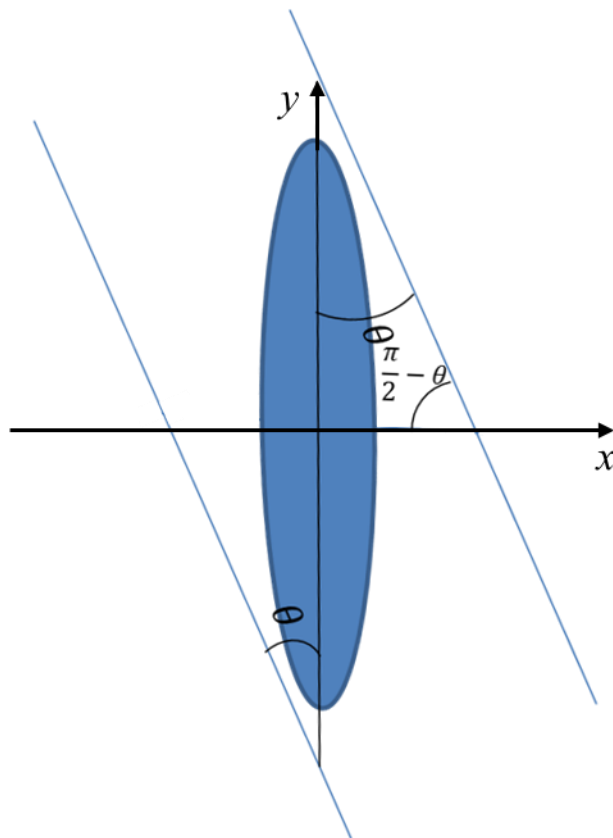


Figure 4: The yellow, green, blue, orange and red full circles indicate the locations on the surface of the finger pad subtended by the angle u corresponding to 0° , 30° , 45° , 60° and 90° .



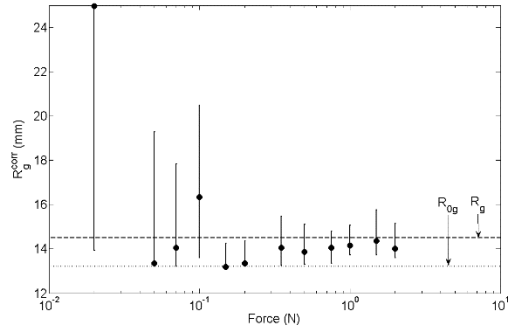
Radial face



Rotated and repositioned

Figure 5: Upper - schematic diagram showing the radial face view of the finger pad ellipsoid resting on the wedge. Lower - rotation and repositioning of the geometry to set the x - y axes as the palmar-distal axes and the centre of the ellipsoid located at the origin.

a)



b)

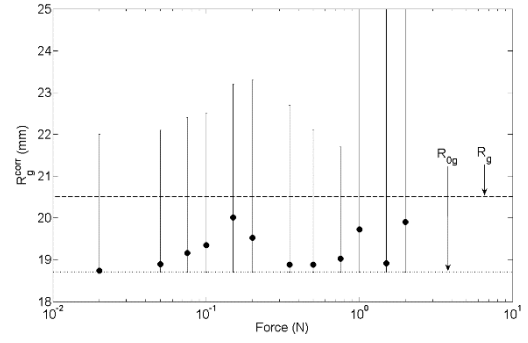


Figure 6: Corrected geometric radii, R_g^{corr} , obtained from Eqn. 1 using Eqn. 2 are plotted as solid dots as a function of normal load for wedge angles of a) 45° and b) 30° . The error bars are obtained from a sensitivity analysis although the geometric radius is assumed exact. The effective radius from the experimental contact compliance was determined in the manuscript and is denoted by the dashed line, and labelled as R_g . The dotted line is the mean radius of curvature obtained from the undeformed geometry and is labelled as R_{0g} .